Computers & Industrial Engineering 78 (2014) 205–212

Contents lists available at ScienceDirect

Computers & Industrial Engineering

journal homepage: www.elsevier.com/locate/caie

A new exponentially weighted moving average control chart for monitoring the coefficient of variation ☆

Jiujun Zhang [a], Zhonghua Li [b], Bin Chen [c], Zhaojun Wang [b,*]

[a] Department of Mathematics, Liaoning University, Shenyang 110036, PR China
[b] LPMC and Institute of Statistics, Nankai University, Tianjin 300071, PR China
[c] School of Mathematics and Statistics, Jiangsu Normal University, Xuzhou 221116, PR China

ARTICLE INFO

Article history:
Received 10 April 2014
Received in revised form 27 July 2014
Accepted 28 September 2014
Available online 22 October 2014

Keywords:
Coefficient of variation
Exponentially weighted moving average
Average run length
Statistical Process Control

ABSTRACT

Monitoring coefficient of variation is one of the successful approaches to Statistical Process Control (SPC) when the process mean and standard deviation are not constants. This paper presents a modified Exponentially Weighted Moving Average (EWMA) chart in order to further enhance the sensitivity of the EWMA control chart proposed by Castagliola et al. (2011). Tables are provided for the statistical properties of the new chart. Some numerical results and comparisons are given and show that the new chart has an average run length performance that is superior to some other competing procedures. A real data example from manufacturing shows that it performs quite well in applications.

1. Introduction

Ever since Shewhart introduced control charts, it has become a common practice for practitioners to use various control charts to monitor different processes. When we deal with variable data, the charting technique usually employs a chart to monitor the process mean and another chart to monitor the process variance. The Shewhart $\overline{X}$ and S (or R) charts are industry standards for quality control applications where the mean μ and the standard deviation σ of a process must be statistically controlled at the nominal values μ_0 and σ_0. The baseline assumption is that the nominal values are fixed constants, and there are indeed many applications for which this assumption is reasonable. To this end, it is reasonable to monitor the process mean and variance simultaneously by a single chart, see Zhang, Zou, and Wang (2010, 2011), Costa and Machado (2013), Du, Huang, and Lv (2013) and Menzefricke (2013a, 2013b). However, control charting techniques were recently extended to various service sectors such as health, education, finance (see Sharpe, 1994) and various societal applications. In addition, it is also adopted in chemical and biological assay quality control to validate results, where the mean and the standard deviation may not be constants all the time and the process may nevertheless be declared in-control if their ratio remains stable around a constant value, see Reed, Lynn, and Meade (2002). As stated by Castagliola, Achouri, Taleb, Celano, and Psarakis (2013a, 2013b), there are many opportunities for SPC monitoring of the coefficient of variation (CV) also in the fields of materials engineering and manufacturing. Tool cutting life and several properties of sintered materials are typical examples from this setting, and hence we will show our proposed scheme performs quite well in applications through a real data example from sintered materials manufacturing. In this case, the routine use of the Shewhart charts is dubious, even though statistical control is still sought. For example, direct proportionality $\sigma = \gamma\mu$ is a common relationship between the mean and standard deviation in some processes. In this less restrictive setting, μ and σ may vary in the parameter space subject only to $\gamma = \frac{\sigma}{\mu}$, so that only the CV parameter, γ, is constant. In this case, it is natural to explore the use of the CV. Several published works have investigated the distribution of sample CV and its related inferential properties, see Hendricks and Robey (1996), Iglewicz, Myers, and Howe (1968), Mckay (1932), Mahmoudvand and Hassani (2009), Reh and Scheffler (1996), Tian (2005), Vangel (1996) and Verrill and Johnson (2007).

Recently, Kang, Lee, Seong, and Hawkins (2007) developed a Shewhart-Type control chart for monitoring the cyclosporine level in organ-transplantation procedures using rational subgroups. As stated by Kang et al. (2007), the advantage of adopting $\hat{\gamma}$ as the monitored statistic by a control chart is evident for those chemical or physical processes for which the variation of a quality characteristic X has to be controlled and the population standard deviation σ is proportional to the mean μ. This Shewhart-Type chart is sensi-

☆ This manuscript was processed by Area Editor Min Xie.

* Corresponding author. Tel.: +86 22 23498233; fax: +86 22 23506423.
E-mail addresses: zjjly790816@163.com (J. Zhang), zli@nankai.edu.cn (Z. Li), bchen@jsnu.edu.cn (B. Chen), zjwang@nankai.edu.cn (Z. Wang).

http://dx.doi.org/10.1016/j.cie.2014.09.027
0360-8352/

tive to large shifts but not sensitive to small to moderate shifts. The EWMA chart is also a good alternative to the Shewhart control chart when we are interested in detecting small shifts. The performance of the EWMA control chart is approximately equivalent to that of the cumulative sum (CUSUM) control chart, and in some ways it is easier to set up and operate. To this end, Hong, Kang, Baek, and Kang (2008) proposed an EWMA-CV control chart in order to improve the Shewhart-type chart proposed by Kang et al. (2007) and detect small shifts more efficiently.

Castagliola, Celano, and Psarakis (2011) suggested a new method to monitor the CV by means of two one-sided EWMA charts of the CV squared. A numerical analysis demonstrated that this chart almost always performed better than the control chart proposed by Hong et al. (2008) even if this statistical outperformance is often rather small. However, the authors did not investigate the simultaneous monitoring of increasing or decreasing shifts in CV, which is important in real applications.

Recently, Calzada and Scariano (2013) developed a synthetic control chart for monitoring the CV. The results showed that the synthetic chart performed better than that of Kang et al. (2007), but worse than Castagliola et al. (2011) as long as the increasing shift in the CV is not too large. In addition, Castagliola et al. (2013a) evaluated an adaptive Shewhart control chart implementing variable sampling interval strategy to monitor the process CV. Castagliola et al. (2013b) proposed a Shewhart chart with supplementary run rules to monitor the CV. However, as they pointed out, the run rules charts for monitoring the CV does not outperform more advanced strategies like the chart proposed by Castagliola et al. (2011) or the synthetic chart proposed by Calzada and Scariano (2013).

The goal of this paper is to improve the performance of EWMA$_{-\gamma^2}$ chart based on the preliminary work of Castagliola et al. (2011) by proposing a new strategy for monitoring the coefficient of variation. The remainder of this paper is organized as follows. A brief review of the one-sided EWMA$_{-\gamma^2}$ chart of Castagliola et al. (2011) is given in Section 2. Following that, our modified EWMA chart is presented and the statistical performance of the new chart is investigated. Sets of optimal design parameters are also provided for different values of the in-control coefficient of variation, for different sample sizes, and for a wide range of deterministic shifts, including both decreasing and increasing cases in this section. The numerical comparisons with some other procedures are carried out in Section 3. The application of our proposed method is illustrated in Section 4 by a real data example from chemical process control. Several remarks conclude this paper in Section 5.

Now we summarize some abbreviated expressions used in this paper for easy reference and recapitulation.

- EWMA: Exponentially Weighted Moving Average; Cusum: cumulative sum.
- CV: coefficient of variation;
  MCV: modified chart for monitoring CV (this paper proposed);
  ECV: EWMA chart for monitoring CV (Castagliola et al., 2011);
  SynCV: synthetic chart for monitoring CV (Calzada & Scariano, 2013);
  SRCV: Shewhart chart with supplementary run rules for monitoring CV (Castagliola et al., 2013b);
- UCL: upper control limit; LCL: lower control limit; UWL: upper warning limit; LWL: lower warning limit;
- IC: in-control; OC: out-of-control;
- ARL: average run length; ZS-ARL: zero-state average run length; SDRL: standard deviation of the run length.

2. Monitoring CV with new modified EWMA chart

Suppose that we observe subgroups $X_{k1}, X_{k2}, \ldots, X_{kn}$ of size n at times $k = 1, 2, \ldots$. We also assume that there is independence within and between these subgroups and each random variable X_{kj} follows a normal $N(\mu_k, \sigma_k)$ distribution, where parameters μ_k and σ_k are constrained by the relation $\gamma_k = \frac{\mu_k}{\sigma_k} = \gamma_0$ when the process is in control. This implies that, from one subgroup to another, the values of μ_k and σ_k may change, but the coefficient of variation $\gamma_k = \frac{\mu_k}{\sigma_k}$ must be equal to some predefined in-control value γ_0, common to all the subgroups.

2.1. A brief review of EWMA$_{-\gamma^2}$ chart (Castagliola et al., 2011)

In this subsection, we give a brief review of the EWMA$_{-\gamma^2}$ chart proposed by Castagliola et al. (2011) (denoted as ECV chart). First, an upward ECV chart aims to detect an increase in the CV and is defined as

$$Z_k^+ = \max(\mu_0(\hat{\gamma}^2), (1-\lambda^+)Z_{k-1}^+ + \lambda^+ \hat{\gamma}_k^{\,2}), \tag{1}$$

with $Z_0^+ = \mu_0(\hat{\gamma}^2)$ as the initial value and with the asymptotic corresponding upper control limit (UCL)

$$UCL = \mu_0(\hat{\gamma}^2) + K^+ \sqrt{\frac{\lambda^+}{2-\lambda^+}\sigma_0(\hat{\gamma}^2)}. \tag{2}$$

Second, a downward ECV chart aims to detect a decrease in the CV and is defined as

$$Z_k^- = \min(\mu_0(\hat{\gamma}^2), (1-\lambda^-)Z_{k-1}^- + \lambda^- \hat{\gamma}_k^{\,2}), \tag{3}$$

with $Z_0^- = \mu_0(\hat{\gamma}^2)$ and with the asymptotic corresponding lower control limit (LCL)

$$LCL = \mu_0(\hat{\gamma}^2) + K^- \sqrt{\frac{\lambda^-}{2-\lambda^-}\sigma_0(\hat{\gamma}^2)}, \tag{4}$$

where $\mu_0(\hat{\sigma}^2)$ and $\sigma_0(\hat{\sigma}^2)$ are the mean and standard deviation of $\hat{\gamma}^2$ when the process is in control and $\lambda^+(\lambda^-)$ and $K^+(K^-)$ are the smoothing constant and chart coefficient of the upward (downward) ECV chart. Approximations for $\mu_0(\hat{\sigma}^2)$ and $\sigma_0(\hat{\sigma}^2)$ are provided by Breunig (2001) as

$$\mu_0(\hat{\gamma}^2) = \gamma_0^2\left(1 - \frac{3\gamma_0^2}{n}\right), \tag{5}$$

and

$$\sigma_0(\hat{\gamma}^2) = \left\{\gamma_0^4\left(\frac{2}{n-1} + \gamma_0^2\left(\frac{4}{n} + \frac{20}{n(n-1)} + \frac{75\gamma_0^2}{n^2}\right)\right) - \left(\mu_0(\hat{\sigma}^2) - \gamma_0^2\right)^2\right\}^{\frac{1}{2}}. \tag{6}$$

The suggested one-sided EWMA charts have many advantages according to Castagliola et al. (2011). However, it should be noted that, in Eq. (1), when $\mu_0(\hat{\gamma}^2) > (1-\lambda^+)Z_{k-1}^+ + \lambda^+\hat{\gamma}_k^{\,2}$, then $Z_k^+ = \mu_0(\hat{\gamma}^2)$. So, in the next time point, we have

$$Z_{k+1}^+ = \max(\mu_0(\hat{\gamma}^2), (1-\lambda^+)\mu_0(\hat{\gamma}^2) + \lambda^+\hat{\gamma}_{k+1}^2). \tag{7}$$

It is obvious that the samples collected before time $k+1$ are not used any longer. However, the advantage of the EWMA chart is that it will use not only the information of the current sample but also will use the former samples. To this end, in order to improve the performance of the ECV chart, next, we propose a modified EWMA chart based on the ECV chart. The comparison results showed that the new chart performs much better than the ECV chart, especially for detecting small to moderate shifts in CV.

2.2. Our modified methodology

To further enhance the sensitivity of the ECV chart in monitoring the process CV, we propose a modified procedure to the construction of Z_k^+ and Z_k^-. First, we define a new upward EWMA

chart based on the sample CV (denoted as upward MCV chart), $\hat{\gamma}_k^2$, as follows:

$$Z_k^+ = \max(\mu_0(\hat{\gamma}^2), U_k^+), \tag{8}$$

where U_k^+ is defined as

$$U_k^+ = (1-\lambda^+)U_{k-1} + \lambda^+\hat{\gamma}_k^2, \tag{9}$$

where $U_0^+ = \mu_0(\hat{\gamma}^2)$ as the initial value. The asymptotic corresponding UCL is the same as defined in Eq. (2). Note that the difference between the MCV and the ECV charts is that our new chart will use not only the information of the current sample but also will use all of the former samples. So, it is expected that the new chart will be more effective than the ECV chart.

Second, a new downward EWMA chart based on the sample CV (denoted as downward MCV chart), $\hat{\gamma}_k^2$, as follows:

$$Z_k^- = \max(\mu_0(\hat{\gamma}^2), U_k^-), \tag{10}$$

where U_k^- is defined as

$$U_k^- = (1-\lambda^-)U_{k-1} + \lambda^-\hat{\gamma}_k^2, \tag{11}$$

where $U_0^- = \mu_0(\hat{\gamma}^2)$ as the initial value. The asymptotic corresponding LCL is the same as defined in Eq. (4).

An alarm is triggered as soon as $Z_k^+ > UCL$ or $Z_k^- < LCL$, respectively. A combination of the two one-sided charts can be implemented to detect both increase and decrease shifts in CV. The K values of the upper and lower charts for some combinations of λ, γ_0 and n are presented in Tables 1 and 2 when the in control average run length (IC-ARL) is 370. Upon request, Fortran programs that optimize our new CV chart for other parameter conditions will be provided.

3. Numerical results and comparison

In this paper, the average run length (ARL) measures the efficiency of a control chart in detecting a process change. This ARL performance is usually referred to as the zero-state ARL(ZS-ARL) performance.When the process is in control, it is desirable that the expected number of samples, in-control ARL(IC-ARL), taken since the beginning of the monitoring until a signal is large, to guarantee few false alarms. When the process is out of control, it is desirable that the expected number of samples, out-of-control ARL(OC-ARL), taken since the occurrence of the assignable cause until a signal is small, in order to guarantee fast detection of process changes. A control chart is considered better than its competitors if it has the smaller OC-ARL value for a specific shift τ^* in CV when IC-ARL is the same for all the charts. In this section, the performance of our new chart is compared with some competing charts, including the ECV chart, the synthetic CV chart and the Shewhart chart with supplementary run rules, respectively.

Table 1
K^+ values of the upper MCV chart for the selected combinations of λ, γ_0 and n when IC-ARL = 370.

n	γ_0	$\lambda = 0.05$	0.1	0.2	0.3	0.5
5	0.05	2.363	2.793	3.254	3.555	3.962
	0.10	2.439	2.851	3.311	3.613	4.023
	0.15	2.568	2.964	3.408	3.711	4.131
	0.20	2.759	3.110	3.555	3.857	4.287
7	0.05	3.322	2.725	3.135	3.398	3.743
	0.10	2.390	2.773	3.188	3.447	3.798
	0.15	2.509	2.866	3.269	3.525	3.879
	0.20	2.666	2.998	3.379	3.633	4.009
10	0.05	2.29	2.666	3.037	3.262	3.555
	0.10	2.352	2.715	3.077	3.301	3.599
	0.15	2.451	2.791	3.144	3.371	3.667
	0.20	2.585	2.901	3.237	3.456	3.766
15	0.05	2.266	2.617	2.949	3.149	3.398
	0.10	2.309	2.656	2.983	3.184	3.437
	0.15	2.393	2.715	3.042	3.232	3.486
	0.20	2.505	2.801	3.110	3.306	3.565

Table 2
K^- values of the lower MCV chart for the selected combinations of λ, γ_0 and n when IC-ARL = 370.

n	γ_0	$\lambda = 0.05$	0.1	0.2	0.3	0.5
5	0.05	1.909	2.024	2.002	1.920	1.736
	0.10	1.826	1.963	1.956	1.879	1.703
	0.15	1.699	1.865	1.879	1.814	1.648
	0.20	1.528	1.732	1.777	1.725	1.575
7	0.05	1.950	2.092	2.102	2.043	1.892
	0.10	1.875	2.036	2.062	2.006	1.861
	0.15	1.767	1.951	1.992	1.949	1.813
	0.20	1.616	1.834	1.904	1.873	1.747
10	0.05	1.982	2.148	2.189	2.148	2.029
	0.10	1.924	2.105	2.153	2.119	2.002
	0.15	1.826	2.026	2.095	2.068	1.960
	0.20	1.697	1.924	2.016	2.002	1.902
15	0.05	2.016	2.197	2.266	2.248	2.158
	0.10	1.965	2.158	2.236	2.221	2.136
	0.15	1.885	2.097	2.192	2.180	2.099
	0.20	1.775	2.012	2.122	2.121	2.049

3.1. ARL optimization for the new chart and the comparison with ECV chart

Assume that when the process is in-control, $\gamma = \gamma_0$ and when the process is out-of-control, $\gamma = \gamma_1 = \tau\gamma_0$. Values of $0 < \tau < 1$ correspond to a decrease of the nominal coefficient of variation, while values of $\tau > 1$ correspond to an increase of the nominal coefficient of variation. An optimization philosophy will be considered in this study. In the standard optimization procedure, two special ARL cases merit special attention: the in-control case IC-ARL and out-of-control case OC-ARL, for specified γ_1. Once consideration is given to the cost of halting a stable process to investigate a false-alarm signal, the chart designer specifies IC-ARL at an acceptable level. Next, consideration is given to the magnitude of a shift in the CV, $\gamma = \tau\gamma_0$, regarded as most detrimental to process quality, which must be identified and eliminated as soon as possible. An optimal modified CV chart would minimize the ARL at this shift, τ^*, subject to the chosen in-control ARL constraint. That is, optimal values (λ^*, K^*) are given by

$$(\lambda^*, K^*) = \arg\min_{(\lambda,K)} ARL(\gamma_0, \gamma_1, \lambda, K, n), \tag{12}$$

subject to the constraint

$$ARL(\gamma_0, \gamma_0, \lambda^*, K^*, n) = ARL_0. \tag{13}$$

Similar to Castagliola et al. (2011), the complete heuristic design procedure is implemented as follows:

- when the process is functioning at the nominal coefficient of variation $\gamma = \gamma_0$, then $ARL = ARL_0$, where ARL_0 is some predefined IC-ARL value.
- for a specified value $\gamma = \tau^*\gamma_0 \neq \gamma_0$, the couple (λ^*, K^*) yields the smallest possible OC-ARL.

We compare our new chart with ECV chart in terms of the OC-ARL. The ECV chart introduced by Castagliola et al. (2011) is statistically more efficient at detecting small process shifts than

the regular Shewhart control chart. For fair comparisons, the values of λ^* is always kept larger than 0.05 in order to be consistent with Castagliola et al. (2011). Tables 3 and 4 compare selected OC-ARLs for the one-sided ECV chart and the new chart, where all charts have an IC-ARL of 370 and have been optimized to minimize OC-ARLs at shift τ^*. The optimal couples (λ^*, K^*) for the new charts are presented in the first row of each block of Tables 3 and 4, for $n = \{5, 7, 10, 15\}, \gamma_0 = \{0.05, 0.1, 0.15, 0.2\}$, and $\tau^* = \{0.5, 0.65, 0.8, 0.9\}$ (i.e. decreasing case), $\tau^* = \{1.1, 1.25, 1.5, 2.\}$ (i.e. increasing case), while the out-of-control ZS-ARLs of the MCV(left side) and ECV (right side) charts are presented in the second row of each block. In general, the run length distribution of a control chart can be explored by integral equations, Markov Chain or by a Monte Carlo simulation (Li, Zou, Gong, & Wang, 2014). In this study, we used the Monte Carlo simulation approach through an algorithm developed in FORTRAN.

It can be seen that, whatever the values of n, γ_0 or τ^*, the ARLs of the new chart are smaller than the ARLs of the ECV chart, especially for detecting small to moderate shifts in CV, clearly demonstrating the outperformance of the former over the latter. For instance, concerning the increasing case, if $n = 5, \gamma_0 = 0.1$ and the critical shift is $\tau^* = 1.1$, then OC-ARL in this case are 44.5 for the MCV chart and 51.5 for the ECV chart. Concerning the decreasing case, if $n = 10, \gamma_0 = 0.2$ and the critical shift is $\tau^* = 0.9$ then the OC-ARL is 24.8 for the MCV chart, while, for the ECV chart, the corresponding value of OC-ARL is 31.7. When the shift size is large (e.g., $\tau^* = 1, 5, 2.0$), these two charts have similar performance.

The standard deviation of the run length (denoted as SDRL) is usually used as another measure to evaluate the performance of control charts. The smaller the values of SDRL, the better the performance of a control chart. Computation of SDRLs for both the MCV and ECV charts also demonstrates that the MCV run-length distribution is always more underdispersed than the one corresponding to the ECV chart. For instance, concerning the two examples described above, the SDRL corresponding to the increasing case is 35.9 for the MCV chart, while it is 41.2 for the ECV chart, and the SDRL corresponding to the decreasing case is 15.2 for the MCV chart while it is 19.2 for the ECV chart.

In addition, it is observed from Tables 3 and 4 that the run length profiles for the two charts are highly influenced by the sample size but not strongly influenced by the size of the in-control γ_0, an observation also made by Kang et al. (2007). Under the fixed sample size rational subgrouping model, practitioners of these charts should choose the largest sample size that resources allow.

As noted by Castagliola et al. (2011), specifying this shift a priori is often too restrictive because the quality practitioner may not have historical knowledge of the process, or because shifts are not deterministic but follow some unknown distribution. If the practitioner pre-specifies a shift τ^*, and uses the corresponding optimal parameters but experiences a different shift in the CV, then the run length performance of the chart may be seriously undermined. Castagliola et al. (2011) suggested an alternate optimization procedure in order to cope with the random shift-size problem in the design of control charts monitoring the sample CV. Similar approaches have been proposed by Reynolds and Stoumbos (2004), Wu, Yang, Jiang, and Khoo (2008), and Celano (2009).

From Tables 5 and 6 of Castagliola et al. (2011), we can see that the optimal value of λ is 0.05 when the sample size $n \leqslant 10$ and the charts with $\lambda = 0.1$ perform better for larger sample size. To this end, for simplicity, in this paper, we will not consider the optimi-

Table 3
Optimal couples(λ^*, K^*) and zero-state OC-ARLs of the MCV and ECV charts when IC-ARL = 370.

τ^*	$\gamma_0 = 0.05$	$\gamma_0 = 0.1$	$\gamma_0 = 0.15$	$\gamma_0 = 0.2$
$n = 5$				
0.50	(0.35, 1.875)	(0.33,1.853)	(0.39, 1.741)	(0.43, 1.629)
	(4.5, 4.8)	(4.5, 4.8)	(4.4, 4.8)	(4.4, 4.8)
0.65	(0.21, 1.995)	(0.19, 1.961)	(0.18, 1.885)	(0.16, 1.781)
	(7.9, 8.7)	(7.9, 8.8)	(7.9, 8.8)	(7.8, 8.8)
0.80	(0.07, 1.982)	(0.05, 1.828)	(0.05, 1.699)	(0.05, 1.528)
	(17.8, 20.6)	(17.6, 20.6)	(17.2, 20.7)	(16.3, 20.9)
0.90	(0.05, 1.914)	(0.05, 1.831)	(0.05, 1.699)	(0.05, 1.523)
	(43.9, 52.8)	(43.4, 54.1)	(42.5, 54.3)	(41.1, 55.4)
1.10	(0.05, 2.363)	(0.05, 2.439)	(0.05, 2.578)	(0.05, 2.759)
	(44.1, 51.2)	(44.5, 51.5)	(46.3, 51.9)	(48.5, 52.4)
1.25	(0.08, 2.656)	(0.08, 2.722)	(0.07, 2.759)	(0.09, 3.056)
	(13.5, 15)	(13.7, 15.2)	(14.2,15.4)	(14.8, 15.9)
1.50	(0.15, 3.051)	(0.15, 3.115)	(0.16, 3.256)	(0.14, 3.305)
	(5.3, 5.7)	(5.4, 5.8)	(5.6, 5.9)	(5.8, 6.1)
2.00	(0.31, 3.579)	(0.31, 3.637)	(0.23, 3.510)	(0.2, 3.545)
	(2.3, 2.4)	(2.3, 2.4)	(2.4, 2.5)	(2.5, 2.6)
$n = 7$				
0.50	(0.45, 1.931)	(0.55, 1.821)	(0.46, 1.841)	(0.45, 1.779)
	(3.3, 3.4)	(3.3, 3.4)	(3.3, 3.5)	(3.3, 3.5)
0.65	(0.29, 2.049)	(0.24, 2.043)	(0.22, 1.987)	(0.21, 1.901)
	(5.8, 6.4)	(5.9, 6.4)	(5.9, 6.4)	(5.9, 6.5)
0.80	(0.11, 2.102)	(0.09, 2.023)	(0.09, 2.021)	(0.05, 13.0)
	(13.5, 15.3)	(13.4, 15.4)	(13.4, 15.5)	(13.0, 15.6)
0.90	(0.05, 1.953)	(0.05, 1.882)	(0.05, 1.767)	(0.05, 1.614)
	(33.9, 40.3)	(33.4, 40.7)	(32.7, 41.0)	(32.0, 41.6)
1.10	(0.05, 2.324)	(0.05, 2.392)	(0.05, 2.509)	(0.05, 2.666)
	(34.0, 39.2)	(34.6, 39.4)	(35.8, 40.3)	(37.5, 41.0)
1.25	(0.11, 2.773)	(0.08, 2.656)	(0.11, 2.92)	(0.12, 3.086)
	(10.2, 11.3)	(10.5, 11.4)	(10.7, 11.7)	(11.1, 12)
1.50	(0.21, 3.164)	(0.13, 2.930)	(0.17, 3.164)	(0.15, 3.213)
	(4.0, 4.3)	(4.2, 4.3)	(4.2, 4.4)	(4.4, 4.6)
2.00	(0.25, 3.277)	(0.35, 3.555)	(0.55, 3.945)	(0.35, 3.75)
	(1.8, 1.8)	(1.8, 1.8)	(1.8, 1.9)	(1.9, 2.0)

Table 4
Optimal couples (λ^*, K^*) and zero-state OC-ARLs of the MCV and ECV charts when IC-ARL = 370.

τ^*	$\gamma_0 = 0.05$	$\gamma_0 = 0.1$	$\gamma_0 = 0.15$	$\gamma_0 = 0.2$
$n = 10$				
0.50	(0.53, 2.009)	(0.55, 1.971)	(0.55,1.931)	(0.58, 1.854)
	(2.4, 2.5)	(2.4, 2.5)	(2.4, 2.5)	(2.4, 2.5)
0.65	(0.35, 2.124)	(0.34, 2.099)	(0.35, 2.046)	(0.28, 2.006)
	(4.3, 4.6)	(4.3, 4.6)	(4.3, 4.7)	(4.4, 4.7)
0.80	(0.13, 2.177)	(0.14, 2.138)	(0.12, 2.058)	(0.12, 1.963)
	(10.1, 11.3)	(10.1, 11.4)	(10.1, 11.5)	(10.0, 11.6)
0.90	(0.05, 1.982)	(0.05, 1.926)	(0.05, 1.828)	(0.05, 1.697)
	(25.6,30.6)	(25.6, 30.9)	(25.2, 31)	(24.8, 31.7)
1.10	(0.05, 2.295)	(0.05, 2.353)	(0.05, 2.451)	(0.06, 2.656)
	(26.0, 30.2)	(26.5, 30.4)	(27.5, 31.0)	(28.7, 31.4)
1.25	(0.12, 2.764)	(0.14, 2.885)	(0.16, 3.022)	(0.12, 2.983)
	(7.7, 8.4)	(7.8, 8.5)	(8.0, 8.7)	(8.4, 9.0)
1.50	(0.25, 3.160)	(0.21, 3.107)	(0.19, 3.116)	(0.21, 3.261)
	(3.0, 3.2)	(3.1, 3.2)	(3.2, 3.3)	(3.3, 3.4)
2.00	(0.32, 3.301)	(0.37, 3.427)	(0.25, 3.266)	(0.36, 3.569)
	(1.4, 1.4)	(1.4, 1.4)	(1.5, 1.5)	(1.5, 1.5)
$n = 15$				
0.50	(0.75, 2.031)	(0.75, 2.009)	(0.75, 1.977)	(0.75, 1.931)
	(1.6, 1.6)	(1.7, 1.7)	(1.7, 1.7)	(1.7, 1.7)
0.65	(0.4, 2.209)	(0.41, 2.180)	(0.36, 2.163)	(0.35, 2.109)
	(3.1, 3.3)	(3.1, 3.3)	(3.2, 3.3)	(3.2, 3.3)
0.80	(0.22, 2.266)	(0.16, 2.227)	(0.16, 2.173)	(0.13, 2.071)
	(7.3, 8.1)	(7.4, 8.1)	(7.4, 8.2)	(7.5, 8.3)
0.90	(0.05, 2.012)	(0.05, 1.963)	(0.05, 1.885)	(0.05, 1.777)
	(19.4, 22.7)	(19.4, 22.8)	(19.2, 23)	(18.9, 23.4)
1.10	(0.05, 2.266)	(0.06, 2.402)	(0.06, 2.481)	(0.06, 2.583)
	(19.6, 22.4)	(20.0, 22.7)	(20.5, 23.2)	(21.4, 23.7)
1.25	(0.19, 2.929)	(0.19, 2.961)	(0.19, 2.901)	(0.17, 3.037)
	(5.6, 6.1)	(5.7, 6.2)	(5.9, 6.3)	(6.1, 6.5)
1.50	(0.33, 3.201)	(0.25, 3.086)	(0.31, 3.252)	(0.3, 3.305)
	(2.2, 2.3)	(2.3, 2.3)	(2.3, 2.4)	(2.4, 2.5)
2.00	(0.65, 3.525)	(0.25, 3.086)	(0.31, 3.252)	(0.4, 3.451)
	(1.1, 1.1)	(1.2, 1.2)	(1.2, 1.2)	(1.2, 1.2)

zation procedure mentioned above, instead, we make a comparison between the MCV and ECV charts with $\lambda = 0.05, 0.1$ and $\gamma_0 = 0.1, 0.2$. The results are summarized in Table 5. From this table it is observed that the MCV chart always yielded smaller ARL values than the ECV chart, especially for detecting small to moderate shifts in CV.

3.2. Comparison with the synthetic chart

Very recently, Calzada and Scariano (2013) suggested a synthetic control chart (SynCV in short) for monitoring the CV. Since the original synthetic chart to be compared in this section are designed to monitor increases in γ, we will only compare the upward modified CV chart with the synthetic chart in this paper. We compared the behavior of the proposed chart for two sizes of rational groups, $n = 5$ and $n = 10$. These choices are widely recommended and used in rational group cases. All charts have an IC-ARL of 370.4 and the synthetic and our new CV charts have been optimized to minimize OC-ARLs at shift $\tau^* = 1.25, 1.50$ and 2.00, respectively. The results are tabulated in Tables 6 and 7. From these two tables we observed the following results:

- When the sample size $n = 5$, the new chart outperforms the synthetic chart in almost all cases except when the shift size is large (e.g., $\tau = 2$). For instance, when $\gamma_0 = 0.1, \tau = 1.25$ and $\tau^* = 1.25$. Calzada and Scariano (2013) suggested $(L^*, LCL^*, UCL^*) = (31, 0.02271, 0.19499)$. Table suggests $(\lambda^*, K^*) = (0.08, 2.722)$, the OC-ARL is 24.3 for the synthetic chart, while, for the new chart, the corresponding value of OC-ARL is 13.7. In addition, the computation of SDRLs (not shown

Table 6
OC-ARLs of the MCV and SynCV charts when IC-ARL = 370 and $n = 5$.

τ	$\tau^* = 1.25$		$\tau^* = 1.50$		$\tau^* = 2$	
	MCV	SynCV	MCV	SynCV	MCV	SynCV
$\gamma_0 = 0.05$						
1.00	370	370	370	370	370	370
1.05	107.8	220.2	122.7	228.9	146.9	239.2
1.10	47.5	118.9	54.8	128.3	70.7	141.1
1.15	27.5	65.0	30.6	71.5	39.4	82.0
1.20	18.4	37.9	19.8	41.7	24.8	49.1
1.25	13.5	24.0	14.1	25.9	16.8	30.8
1.30	10.7	16.5	10.8	17.2	12.4	20.4
1.50	5.6	6.3	5.4	5.8	5.5	6.3
2.00	2.6	2.2	2.4	2.1	2.3	2.0
$\gamma_0 = 0.10$						
1.05	108.0	220.5	24.7	229.3	148.9	239.7
1.10	48.2	119.4	55.7	129.0	71.8	141.8
1.15	27.6	65.5	31.2	72.2	40.0	82.7
1.20	18.7	38.3	20.2	42.2	25.1	49.6
1.25	13.7	24.3	14.5	26.2	17.3	31.2
1.30	10.9	16.7	10.9	17.4	12.6	20.7
1.50	5.8	6.4	5.4	5.9	5.6	6.4
2.00	2.7	2.3	2.5	2.1	2.3	2.0
$\gamma_0 = 0.15$						
1.05	107.3	219.1	128.5	230.5	139.7	240.7
1.10	48.2	118.7	58.3	130.4	65.9	143.2
1.15	28.3	65.3	32.5	73.3	36.6	84.0
1.20	19.2	38.4	21.0	43.0	23.1	50.6
1.25	14.2	24.9	14.9	26.8	16.0	32.0
1.30	11.3	16.9	11.3	17.9	11.9	21.3
1.50	6.0	6.6	5.6	6.0	5.6	6.6
2.00	2.8	2.4	2.5	2.2	2.4	2.1

Table 5
OC-ARLs of the MCV and ECV charts when IC-ARL = 370.

λ	γ_0	τ	$n = 5$		$n = 7$		$n = 10$		$n = 15$	
			MCV	ECV	MCV	ECV	MCV	ECV	MCV	ECV
0.05	0.1	1.00	370	370	370	370	370	370	370	370
		1.05	98.6	113.6	80.2	93.2	63.6	74.3	48.5	56.8
		1.10	44.8	51.2	34.5	39.8	26.7	30.3	20.0	22.7
		1.15	26.7	30.2	20.4	23.3	15.9	17.8	12.0	13.5
		1.20	18.5	20.8	14.3	16.0	11.1	12.4	8.5	9.6
		1.25	13.9	15.6	10.8	12.1	8.5	9.5	6.6	7.3
		1.50	6.1	6.7	4.8	5.3	3.9	4.3	3.1	3.4
		2.00	2.8	3.1	2.3	2.5	1.9	2.1	1.6	1.7
	0.2	1.00	370	370	370	370	370	370	370	370
		1.05	103.9	113.6	84.6	93.6	67.8	75.6	51.7	58.3
		1.10	48.1	52.3	37.2	40.9	28.8	31.7	21.7	23.7
		1.15	29.1	31.2	22.4	24.2	17.3	18.7	13.1	14.3
		1.20	20.3	21.7	15.6	16.9	12.1	13.1	9.3	10.1
		1.25	15.3	16.3	11.9	12.8	9.3	10.0	7.2	7.8
		1.50	6.7	7.1	5.3	5.7	4.2	4.5	3.3	3.6
		2.00	3.1	3.3	2.5	2.7	2.1	2.2	1.7	1.8
0.1	0.1	1.00	370	370	370	370	370	370	370	370
		1.05	112.6	127.0	91.6	105.7	72.8	84.6	55.9	64.3
		1.10	50.1	57.4	37.9	43.7	28.4	32.7	20.8	23.4
		1.15	28.4	32.5	21.2	24.1	15.9	17.8	11.7	12.9
		1.20	18.9	21.2	14.1	15.7	10.7	11.8	7.9	8.7
		1.25	13.4	15.2	10.4	11.4	7.9	8.7	6.0	6.5
		1.50	5.6	6.0	4.4	4.7	3.4	3.7	2.7	2.9
		2.00	2.6	2.7	2.1	2.2	1.7	1.8	1.4	1.5
	0.2	1.00	370	370	370	370	370	370	370	370
		1.05	117.3	129.4	96.6	106.5	77.3	86.6	58.0	66.2
		1.10	52.9	58.6	40.4	44.8	30.4	34.1	21.9	24.3
		1.15	30.2	33.5	22.7	24.8	17.0	18.6	12.4	13.5
		1.20	20.2	21.8	15.2	16.4	11.5	12.4	8.5	9.1
		1.25	14.8	16.0	11.2	12.0	8.6	9.2	6.4	6.9
		1.50	6.0	6.4	4.7	4.9	3.7	3.9	2.9	3.1
		2.00	2.8	2.9	2.1	2.3	1.8	1.9	1.5	1.5

Table 7
OC-ARLs of the MCV and SynCV charts when IC-ARL = 370 and n = 10.

τ	$\tau^* = 1.25$		$\tau^* = 1.50$		$\tau^* = 2$	
	MCV	SynCV	MCV	SynCV	MCV	SynCV
$\gamma_0 = 0.05$						
1.00	370	370	370	370	370	370
1.05	76.3	195.6	96.2	208.2	104.9	218.8
1.10	29.2	84.4	36.8	95.9	41.5	106.7
1.15	15.9	38.0	18.7	44.5	20.7	51.6
1.20	10.5	19.5	11.6	22.6	12.4	26.8
1.25	7.8	11.5	8.0	12.8	8.5	15.3
1.30	6.1	7.6	6.1	8.1	6.3	9.5
1.50	3.3	3.0	3.0	2.7	3.0	2.9
2.00	1.6	1.3	1.5	1.3	1.4	1.2
$\gamma_0 = 0.10$						
1.05	80.3	196.2	91.5	209.4	112.3	219.7
1.10	30.5	85.3	35.0	97.1	44.9	107.8
1.15	16.5	38.6	18.1	45.3	22.7	52.4
1.20	10.7	19.8	11.3	23.1	13.5	27.3
1.25	7.9	11.7	8.0	13.1	9.1	15.6
1.30	6.1	7.8	6.1	8.3	6.6	9.8
1.50	3.3	3.0	3.1	2.8	3.1	3.0
2.00	1.6	1.3	1.5	1.3	1.4	1.2
$\gamma_0 = 0.15$						
1.05	85.0	197.3	90.3	210.6	99.2	221.2
1.10	32.6	86.5	34.6	98.7	38.3	109.7
1.15	17.2	39.4	18.0	46.4	19.6	53.8
1.20	11.1	20.4	11.4	23.8	12.1	28.2
1.25	8.1	12.1	8.1	13.6	8.4	16.2
1.30	6.3	8.1	6.3	8.6	6.4	10.1
1.50	3.3	3.1	3.2	2.9	3.2	3.1
2.00	1.6	1.4	1.6	1.3	1.5	1.3

Table 8
OC-ARLs of the MCV and SRCV charts when IC-ARL = 370 and $\lambda = 0.05$.

n	τ	$\gamma_0 = 0.05$		$\gamma_0 = 0.1$		$\gamma_0 = 0.15$		$\gamma_0 = 0.2$	
		MCV	SRCV	MCV	SRCV	MCV	SRCV	MCV	SRCV
5	0.5	8.4	6.2	8.2	6.2	7.9	6.3	7.5	6.3
	0.6	10.2	11.8	10.0	11.8	9.7	12.0	9.1	12.2
	0.7	13.7	28.4	13.4	28.6	13.0	29.0	12.3	29.5
	0.8	22.3	80.0	21.9	80.6	21.4	81.6	20.5	83.0
	0.9	60.8	236.5	60.3	237.5	59.8	239.3	58.8	241.6
	1.1	61.5	144.5	62.7	145.3	64.4	146.6	67.2	148.4
	1.2	22.7	54.4	23.2	54.9	23.9	55.8	25.3	57.0
	1.5	7.0	11.8	7.1	12.0	7.4	12.2	7.8	12.6
	2.0	3.1	5.6	3.2	5.7	3.3	5.7	3.5	5.9
10	0.5	5.6	4.1	5.5	4.1	5.4	4.1	5.2	4.1
	0.6	6.7	5.0	6.6	5.0	6.5	5.0	6.2	5.1
	0.7	8.7	8.9	8.6	9.0	8.4	9.1	8.1	9.3
	0.8	13.4	26.1	13.3	26.4	13.1	26.9	12.7	27.6
	0.9	33.2	119.1	33.1	120.3	32.9	122.1	32.5	124.6
	1.1	34.0	86.9	34.7	87.7	35.6	89.2	37.3	91.2
	1.2	13.1	25.6	13.4	26.0	13.9	26.6	14.6	27.5
	1.5	4.4	6.2	4.4	6.3	4.6	6.4	4.8	6.6
	2.0	2.1	4.2	2.1	4.3	2.2	4.3	2.3	4.3
15	0.5	4.6	4.0	4.5	4.0	4.4	4.0	4.3	4.0
	0.6	5.4	4.2	5.3	4.2	5.2	4.2	5.1	4.2
	0.7	6.9	5.8	6.8	5.8	6.7	5.9	6.6	6.0
	0.8	10.4	14.4	10.3	14.6	10.2	14.9	10.0	15.3
	0.9	24.5	75.3	24.4	76.2	24.2	77.6	24.0	79.6
	1.1	24.7	60.9	25.3	61.6	26.1	62.9	27.2	64.7
	1.2	9.9	16.6	10.1	16.8	10.5	17.3	11.0	17.9
	1.5	3.4	4.9	3.5	5.0	3.6	5.0	3.8	5.1
	2.0	1.7	4.1	1.7	4.1	1.8	4.1	1.9	4.1

in the Table) for both the synthetic and the new charts also demonstrates that the new chart run-length distribution is always more underdispersed than the synthetic chart. For instance, concerning example described above, the SDRL is 9.3 for the new chart, while it is 30.6 for the synthetic chart.

- When the sample size $n = 10$, the synthetic chart does better when $\tau \geqslant 1.5$, but the difference is not negligible.

The overall conclusion that can be obtained is that our new chart generally has the satisfactory detection performance for various changes in CV. This, again, shows that the new chart is quite a useful tool for practitioners to monitor the CV.

3.3. Comparison with the Shewhart chart with supplementary run rules

Castagliola et al. (2013b) proposed a Shewhart chart with supplementary run rules (SRCV in short) to monitor the CV. They studied three sensitizing rules on Shewhart CV chart, 2-out-of-3, 3-out-of-4 and 4-out-of-5. As they stated, the 4-out-of-5 chart has better performance in most cases, so, we choose this chart as a benchmark in this comparison. Because the SRCV chart is two-sided, in order to make a fair comparison between the two charts, we have computed the OC-ARLs corresponding to two-sided modified CV chart. The smoothing parameter λ is set to 0.05 and the IC-ARL of each of the one-sided chart when used alone is approximately 720 such that the combined chart produces an IC-ARL of 370. Such chart is designed to protect in balance against increasing and decreasing shifts in CV. For comparison purposes, the value of γ_0 and τ considered here are the same as those considered in Castagliola et al. (2013b).

The results of the simulation study are tabulated in Table 8. Concerning the increasing case, the new chart performs always much better than the SRCV chart. For instance, when $n = 10, \gamma_0 = 0.1$ and $\tau = 1.1$ the OC-ARL is 87.7 for the SRCV chart, while, for our new chart, the corresponding value of OC-ARL is 34.7. Concerning the decreasing case, the OC-ARL values in Table 8 are more effective than the SRCV chart except in a very small region where the CV shift is very large. For instance, when $n = 15, \gamma_0 = 0.2$ and $\tau = 0.5$ the OC-ARL is 4.0 for the SRCV chart, while, for our new chart, the corresponding value is 4.3.

We also conduct some simulations for other choices of sample size and IC-ARL, the preceding findings still hold. Generally speaking, the new scheme provides quite a satisfactory performance for various types of shifts including the increase and decrease in CV. By taking the consideration of its easy design and implementation, we think our new proposed scheme is a serious alternative in practical applications.

4. Real data application

In this section, we demonstrate the proposed methodology by a real data set collected from a sintering process manufacturing mechanical parts. This example considers actual data from a sintering process, an operation of powder metallurgy whereby compressed metal powder is heated to a temperature that allows bonding of the individual particles. The process manufactures parts which are required to guarantee a pressure test drop time T_{pd} from 2 bar to 1.5 bar larger than 30 s as a quality characteristic related to the pore shrinkage. Using molten copper to fill pores during the sintering process allows the drop time to be significantly extended. In fact, the larger the quantity Q_C of molten copper absorbed within the sintered compact during cooling, the larger is the expected pressure drop time T_{pd}.

A preliminary regression study relating T_{pd} to the quantity Q_C of molten copper has demonstrated the presence of a constant proportionality $\sigma_{pd} = \gamma_{pd} \times \mu_{pd}$ between the standard deviation of the pressure drop time and its mean. To perform SPC by means

of control charts the quality practitioner decided to monitor the coefficient of variation $\gamma_{pd} = \sigma_{pd}/\mu_{pd}$ in order to detect changes in the process variability. Given the nominal quantity of copper Q_C, a Phase I dataset of $m = 20$ sample data, each having sample size $n = 5$, have been collected; they are listed in Table 7 (top) of Castagliola et al. (2011). The analysis of the Phase I data resulted in an estimate $\gamma_0 = 0.417$ based on a root-mean-square computation and proved that the sintering process is perfectly in-control.

In order to be consistent with Castagliola et al. (2011), τ^* is set to 1.25. The parameters of the new chart which is optimal for detecting a shift from $\gamma_0 = 0.417$ to $\gamma_1 = \gamma_0 \times 1.25 = 0.521$ (i.e. increase of 25%) when $n = 5$ are found by the optimizing algorithm to be $(\lambda^*, K^*) = (0.08, 4.3164)$. Using Eqs. (5) and (6), we have $\mu_0(\hat{\gamma}^2) = 0.1557, \sigma_0(\hat{\gamma}^2) = 0.1643$, and the upper control limit is 0.3005. The Phase I chart (not shown in the paper) seems to confirm that the process is in control.

A second set of data collected during Phase II of the chart implementation are presented in Table 7 (bottom) of Castagliola et al. (2011). These data consist of 20 new samples taken from the process after the occurrence of a special cause increasing process variability. The Z_t and the control limit UCL = 0.3005 are plotted in Fig. 1(a). For comparison, we also plot the ECV and SRCV charts in Fig. 1(b) and (c). From this Figure, it is observed that the our new chart gives an out-of-control signal at observation 13, which is consistent with the result of Castagliola et al. (2011). With the same dataset, the SRCV chart detects an out-of-control signal at the 15th sample, which is two points later than the MCV and ECV charts.

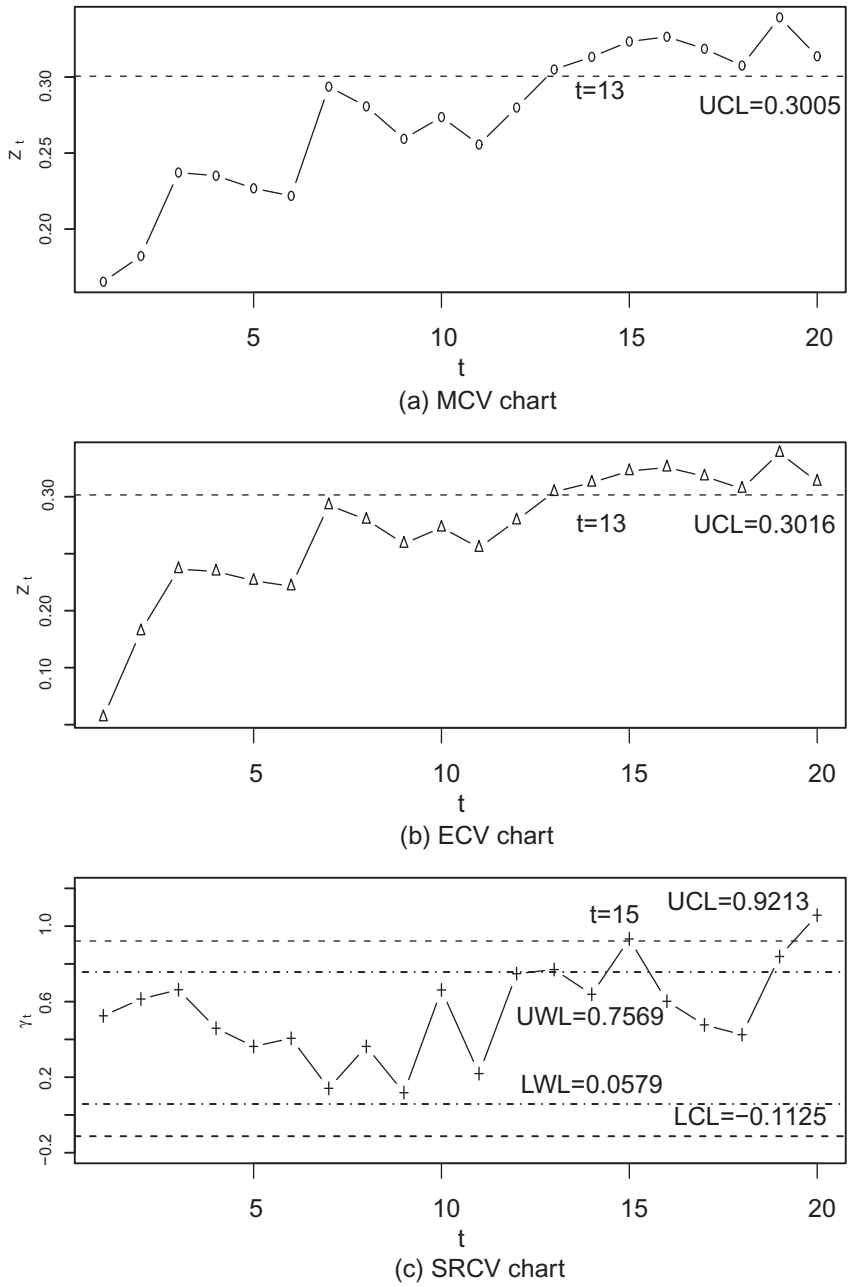

Fig. 1. The MCV, ECV and SRCV charts applied to the sintering process.

5. Summary and conclusion

The CV control chart extends charting capabilities to non-traditional applications. These include situations where the mean is not constant and/or the variance is a function of the mean, so that it may be possible to instead plot the CV to achieve statistical control of that parameter. In this paper, a modified EWMA chart is proposed to monitor the CV in order to further enhance the sensitivity of the EWMA control chart proposed by Castagliola et al. (2011). It is shown that the newly developed control scheme does not only dominate most of the existing charts but is also easy to design and implement as illustrated through an application example of real datasets.

Note that our new chart is based on the assumption that each random variable follows a normal distribution. However, the underlying process is not normal in many applications (Qiu & Li, 2011a, 2011b), and as a result the statistical properties of CV charts can be highly affected in such situations. Hence, it is necessary to check how the proposed methodology performs when the underlying distribution is violated, which also warrants future research. Future research include a self-starting version of the new CV chart and a study of its properties in cases when the IC parameters in the measurement distribution are unknown (Li, Zhang, & Wang, 2010). Moreover, our chart is constructed under statistical design and we believe a control chart for monitoring CV under economic design (Zhang, Xie, Goh, & Shamsuzzaman, 2011) warrants future research.

Acknowledgement

The authors are grateful to the editor, the associate editor and the anonymous referees for their valuable comments that have vastly improved this paper. This research is supported by the Natural Science Foundation of China Grant 11101198, 11201246, 11371202, 11131002, 11431006, 11401573, the start-up funding at Liaoning University, the RFDP of China Grant 20110031110002 and the PAPD of Jiangsu Higher Education Institutions.

Appendix A. Supplementary data

Supplementary data associated with this article can be found, in the online version, at http://dx.doi.org/10.1016/j.cie.2014.09.027.

References

Breunig, R. (2001). An almost unbiased estimator of the coefficient of variation. *Econometric Letters, 70*(1), 15–19.
Calzada, M. E., & Scariano, S. M. (2013). A synthetic control chart for the coefficient of variation. *Journal of Statistical Computation and Simulation, 83*(5), 853–867.
Castagliola, P., Achouri, A., Taleb, H., Celano, G., & Psarakis, S. (2013a). Monitoring the coefficient of variation using a variable sampling interval control chart. *Quality and Reliability Engineering International, 29*(8), 1135–1149.
Castagliola, P., Achouri, A., Taleb, H., Celano, G., & Psarakis, S. (2013b). Monitoring the coefficient of variation using control charts with run rules. *Quality Technology and Quantitative Management, 10*(1), 75–94.
Castagliola, P., Celano, G., & Psarakis, S. (2011). Monitoring the coefficient of variation using EWMA charts. *Journal of Quality Technology, 43*(3), 249–265.
Celano, G. (2009). Robust design of adaptive control charts for manual manufacturing/inspection workstations. *Journal of Applied statistics., 36*, 181–203.
Costa, A. F. B., & Machado, M. A. G. (2013). A single chart with supplementary runs rules for monitoring the mean vector and the covariance matrix of multivariate processes. *Computers & Industry Engineering, 66*(2), 431–437.
Du, S., Huang, D., & Lv, J. (2013). Recognition of concurrent control chart patterns using wavelet transform decomposition and multiclass support vector machines. *Computers & Industry Engineering, 66*(4), 683–695.
Hendricks, W. A., & Robey, W. K. (1996). The sampling distribution of the coefficient of variation. *Annals of Mathematical Statistics, 7*, 129–132.
Hong, E. P., Kang, C. W., Baek, J. W., & Kang, H. W. (2008). Development of CV control chart using EWMA technique. *Journal of the Society of Korea Industrial and Systems Engineering, 31*(4), 114–120.
Iglewicz, B., Myers, R. H., & Howe, R. B. (1968). On the percentage points of the sample coefficient of variation. *Biometrika, 55*(3), 580–581.
Kang, C. W., Lee, M. S., Seong, Y. J., & Hawkins, D. M. (2007). A control chart for the coefficient of variation. *Journal of Quality Technology, 39*(2), 151–158.
Li, Z., Zhang, J., & Wang, Z. (2010). Self-starting control chart for simultaneously monitoring process mean and variance. *International Journal of Production Research, 48*(15), 4537–4553.
Li, Z., Zou, C., Gong, Z., & Wang, Z. (2014). The computation of average run length and average time to signal: an overview. *Journal of Statistical Computation and Simulation, 84*(8), 1779–1802.
Mahmoudvand, R., & Hassani, H. (2009). Two new confidence intervals for the coefficient of variation in a normal distribution. *Journal of Applied Statistics, 36*(4), 429–442.
Mckay, A. T. (1932). Distribution of the coefficient of variation and extended t distribution. *Journal of the Royal Statistical Society, 95*, 695–698.
Menzefricke, U. (2013a). Control charts for the mean and variance based on change point methodology. *Communications in Statistics-Theory and Methods, 42*(6), 988–1007.
Menzefricke, U. (2013b). Combined exponentially weighted moving average charts for the mean and variance based on the predictive distribution. *Communications in Statistics-Theory and Methods, 42*(22), 4003–4016.
Qiu, P., & Li, Z. (2011a). On nonparametric statistical process control of univariate processes. *Technometrics, 53*(4), 390–405.
Qiu, P., & Li, Z. (2011b). Distribution-free monitoring of univariate processes. *Statistics and Probability Letters, 81*(12), 1833–1840.
Reed, G. F., Lynn, F., & Meade, B. D. (2002). Use of coefficient of variation in assessing variability of quantitative assays. *Clinical and Diagnostic Laboratory Immunology, 9*, 1235–1239.
Reh, W., & Scheffler, B. (1996). Significance tests and confidence intervals for coefficients of variation. *Computational Statistics & Data Analysis, 22*(4), 449–452.
Reynolds, J. M. R., & Stoumbos, Z. G. (2004). Control charts and the efficient allocation of sampling resources. *Technometrics, 46*, 200–214.
Sharpe, W. F. (1994). The Sharpe ratio. *Journal of Portfolio Management, 21*, 49–58.
Tian, L. (2005). Inferences on the common coefficient of variation. *Statistics in Medicine, 24*(14), 2213–2220.
Vangel, M. G. (1996). Confidence intervals for a normal coefficient of variation. *American Statistician, 15*, 21–26.
Verrill, S., & Johnson, R. A. (2007). Confidence bounds and hypothesis tests for normal distribution coefficients of variation. *Communications in Statistics-Theory and Methods, 36*(12), 2187–2206.
Wu, Z., Yang, M., Jiang, W., & Khoo, M. B. C. (2008). Optimization designs of the combined Shewhart-CUSUM control charts. *Computational Statistics & Data Analysis, 53*, 496–506.
Zhang, H. Y., Xie, M., Goh, T. N., & Shamsuzzaman, M. (2011). Economic design of time-between-events control chart system. *Computers & Industry Engineering, 60*, 485–492.
Zhang, J., Zou, C., & Wang, Z. (2010). A control chart based on likelihood ratio test for monitoring process mean and variability. *Quality and Reliability Engineering International, 26*, 63–73.
Zhang, J., Zou, C., & Wang, Z. (2011). A new chart for detecting process mean and variability. *Communication in Statistics-Simulation and Computation, 40*, 728–743.